Hole transport in *p*-type ZnO films grown by plasma-assisted molecular beam epitaxy

J. W. Sun
Key Laboratory of Excited State Processes, Changchun Institute of Optics, Fine Mechanics, and Physics, Chinese Academy of Science, Changchun 130033, China and Graduate School of the Chinese Academy of Sciences, Beijing 100049, China

Y. M. Lu[a)]
Key Laboratory of Excited State Processes, Changchun Institute of Optics, Fine Mechanics, and Physics, Chinese Academy of Science, Changchun 130033, China

Y. C. Liu
Center for Advanced Optoelectronic Functional Material Research, Northeast Normal University, Changchun 130024, China

D. Z. Shen, Z. Z. Zhang, B. H. Li, J. Y. Zhang, B. Yao, D. X. Zhao, and X. W. Fan
Key Laboratory of Excited State Processes, Changchun Institute of Optics, Fine Mechanics, and Physics, Chinese Academy of Science, Changchun 130033, China

(Received 17 August 2006; accepted 16 October 2006; published online 4 December 2006)

The hole transport properties of nitrogen doped *p*-type ZnO grown on *c*-plane sapphire (*c*-Al_2O_3) were investigated by temperature-dependent Hall-effect measurements. The experimental Hall mobility was found to be considerably lower than the calculated mobility including ionized impurity scattering, acoustic-mode deformation potential scattering, piezoelectric potential scattering, and polar optical phonon scattering. Atomic force microscopy and x-ray diffraction measurements demonstrated that *p*-type ZnO on *c*-Al_2O_3 consisted of two kinds of 30°-rotated domains surrounded by grain boundaries. Thus, taking the effect of inhomogeneous microstructure on the mobility into account, the calculated mobility agreed favorably with the experimental data. This agreement indicates that besides ionized impurity and acoustic deformation potential scattering at low temperatures and the polar optical phonon scattering at high temperatures, the effects of the inhomogeneous microstructure in *p*-type ZnO films play a more important role in determining the hole mobility. © *2006 American Institute of Physics*. [DOI: 10.1063/1.2398908]

ZnO is a promising material for optoelectronic devices, especially in short-wavelength light emitting diodes (LEDs) and laser diodes.[1] However, the lack of high-quality *p*-type ZnO has hampered the development of ZnO homostructural LEDs. Fortunately, after the prominent progress of ZnO LED by Tsukazaki *et al.*,[2] we have also obtained the reproducible nitrogen (N) doped *p*-type ZnO films grown by plasma-assisted molecular beam epitaxy (P-MBE) on Al_2O_3 using radical NO as oxygen and nitrogen sources,[3] leading to the observation of blue-violet electroluminescence (EL) from a homojunction LED.[4] Recently, many groups have also obtained the EL from ZnO homojunctions using N as the *p*-type dopant.[5,6] Nevertheless, the poor quality of *p*-type films for reported LEDs (hole concentration of 10^{16}–10^{17} cm^{-3}, mobility of 1–10 $cm^2\ V^{-1}\ s^{-1}$ at room temperature) hampered the full realization of ultraviolet EL based on this material. For improving the quality of *p*-type ZnO, it is very important to understand the hole transport properties of these films. However, there are very few efforts focused on the scattering mechanisms of such low hole mobilities.[7,8] Recently, Makino *et al.* have reported the theoretical Hall mobilities for *p*-type ZnO and the comparison of those results with the experimental data.[7] Unfortunately, their calculated Hall mobility is much higher than the experimental data. Thus, more attempts are undoubtedly required to explain the scattering mechanisms of such low mobilities in *p*-type ZnO. In this letter, the hole transport properties of *p*-type ZnO films grown on *c*-Al_2O_3 by P-MBE were studied both experimentally and theoretically. The experimental Hall mobility was found to be considerably lower than the calculated mobility including traditional scattering mechanisms. This discrepancy was favorably explained by the influence of the inhomogeneous microstructure on the hole mobility, including columnar grain size and grain boundaries, which were confirmed by atomic force microscopy (AFM) and x-ray diffraction (XRD) results.

Two typical samples of N-doped ZnO films discussed here, with thicknesses ranging from 400 to 850 nm, were grown on *c*-Al_2O_3 by P-MBE using radical NO as oxygen and nitrogen sources. Temperature-Hall (T-Hall) measurements were carried out by Lakeshore's 7707 system. The crystalline structure was studied by XRD using a Rigaku D/max 2550PC diffractometer.

The *p*-type conduction of N-doped ZnO films was confirmed by T-Hall measurements in the temperature range of 85–300 K. Figure 1 displays the temperature dependence of the hole mobility for samples I and II. It can be seen that there is considerable scatter in the data, which has been explained by errors of the Hall measurements arising from the small magnitude of the Hall mobility.[9,10] Thus, we address this noise issue by repeating the experiments to improve measurement statistics. However, in spite of the scatter, a

[a)]Author to whom correspondence should be addressed; FAX: + 86 431 5682964; electronic mail: ymlu@mail.jl.cn

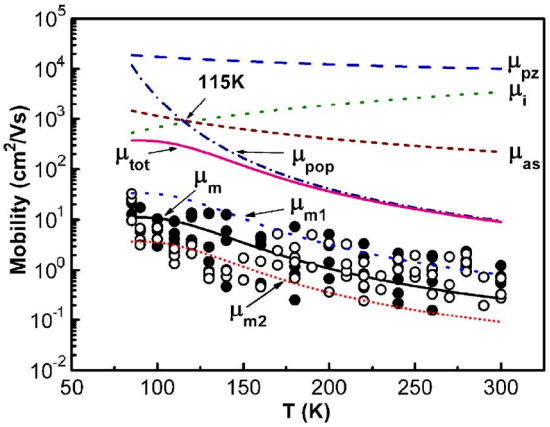

FIG. 1. (Color online) Experimental Hall mobility as a function of temperature for samples I (open circles) and II (closed circles). Also shown by curves are the calculated temperature dependence of the total hole mobility (μ_{tot}) and the the contribution of various scattering mechanisms (μ_i, ionized impurity; μ_{as}, acoustic; μ_{pz}, piezoelectric; μ_{pop}, polar optical). The curve of μ_m is the calculated temperature dependence of the hole mobility for inhomogeneous *p*-type ZnO by Eq. (1).

clear tendency that the hole mobilities for the samples decrease dramatically with increasing temperature can be observed. The highest values $\sim 20\ \mathrm{cm^2\ V^{-1}\ s^{-1}}$ were measured at 85 K for the two samples. With increasing temperature, the mobility values for both samples decrease rapidly and scatter $\sim 1\ \mathrm{cm^2\ V^{-1}\ s^{-1}}$. To understand the hole scattering mechanism in the low-mobility *p*-type ZnO films, the contributions of various scattering mechanisms to the total hole mobility should be considered, such as ionized impurity scattering (μ_i), acoustic-mode deformation potential scattering (μ_{as}), acoustic-mode piezoelectric potential scattering (μ_{pz}), and polar optical phonon scattering (μ_{pop}). To calculate μ_i, μ_{as}, and μ_{pz}, Bolzmann's transport equation was solved by using the universal relaxation time approximation.[11,12] Note that the scattering by polar optical phonons is an inelastic process; Petriz's model was adopted to calculate μ_{pop}.[13,14] The material parameters used in this calculation are summarized in the literature.[9] The effective hole mass was assumed to be $0.64m_0$ (m_0 is the free electron mass), as reported by Look.[9] For the calculation of μ_i, the compensation ratio N_D/N_A should be necessarily considered. Figure 2 shows the temperature dependence of the averaged hole concentration (p) for sample I. Despite the large scatter in high temperatures, N_D/N_A and the activation energy E_A could be deduced by a least-squares fit to the data from 85 to 140 K using Eq. (3) in Ref. 15, as shown in the inset of Fig. 2. The fitted value of N_D/N_A is about 0.11, consistent with that suggested by Look.[16] The calculated hole mobility curves for each scattering mechanism as a function of temperature are shown in Fig. 1. Using Matthiesen's rule, the total hole drift mobility (μ_{tot}) is calculated by combining all of the individual scattering mechanisms above.

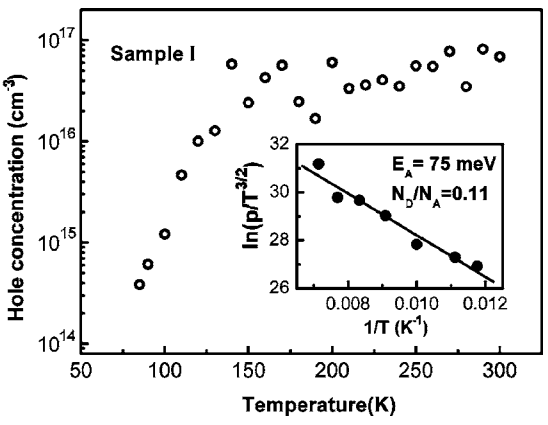

FIG. 2. Temperature dependence of the averaged hole concentration for sample I. The inset is the plot of $\ln(p/T^{3/2})$ vs T^{-1} in the temperature range of 85–140 K.

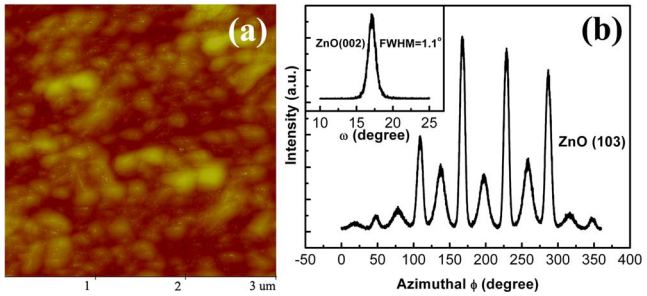

FIG. 3. (Color online) AFM image (a) and XRD Φ scan of the (103) reflection (b) of sample I. The inset of (b) is the ω-scan curve of the (002) reflection for sample I.

As can be seen in Fig. 1, polar optical phonon scattering is the most important mechanism in determining the total hole mobility at high temperatures while ionized impurity and acoustic deformation potential scatterings become dominant at low temperatures. The values of μ_{tot} are 370 and $9\ \mathrm{cm^2\ V^{-1}\ s^{-1}}$ at 85 and 300 K, respectively. It should be noted that the calculated mobility is several tens of times greater than the experimental data for the two samples. Clearly more factors control the hole mobility in *p*-type ZnO films than have been included above. One way that such a factor may arise is from the uncertainties of the material parameters for *p*-type ZnO. However, these uncertainties are not large enough to yield such a great discrepancy between the calculated and experimental data.[17] To clarify this discrepancy, the effect of the microstructure on transport properties should be considered because the mobility can also be lowered by the inhomogeneity of materials.[17]

Figure 3(a) illustrates the AFM image of sample I. It can be seen the film consists of grains with the sizes ranging from 200 to 300 nm, with the surface roughness of 6.3 nm. This implies that the *p*-type films have the columnar structure and incoherent grain boundaries. To further confirm the microstructure of the *p*-type films, XRD θ-2θ scan, (103) Φ-scan, and (002) ω-scan measurements were performed. The θ-2θ scans show that all the *p*-type films exhibit only a (002) diffraction peak with the full width at half maximum (FWHM) of about 0.2° (not shown here), indicating that the films have a high *c*-axis orientation. Figure 3(b) shows the XRD Φ scan of the (103) reflection for sample I. As can be seen, 12 distinct peaks separated by 30°, instead of six peaks for sixfold symmetric single-crystal ZnO, can be observed. This clearly indicates that two kinds of domains are coexisting, rotated by 30° to each other. Shown in the inset of Fig. 3(b) is the ω-scan curve of the (002) reflection with an extremely broad FWHM of about 1.1°, indicating a strong mosaic structure with rotated-domain boundaries and inversion-domain boundaries, consistent with the surface morphology by AFM. These results suggest that *p*-type ZnO films consist of two kinds of 30°-rotated columnar domains surrounded by grain boundaries. Therefore, the influence of the inhomoge-

neity in the *p*-type films on the Hall-effect measurement should be necessarily considered.

Since the pioneer work of Volger[18] for calculating the Hall coefficient in an inhomogeneous material, Bube has given further analysis.[19] However, Bube's paper contains an error in the analysis of the electric field theory. A more reasonable model has been proposed by Heleskivi and Salo[20] They considered the Hall effect in a material consisting of low-resistivity grains (1) (dimension l_1 and resistivity ρ_1) surrounded by thin layers of high resistivity (2) (dimension l_2 and resistivity ρ_2). The measured Hall mobility μ_m can be expressed as

$$\mu_m = \frac{\alpha}{\alpha+\beta}\mu_1, \tag{1}$$

where μ_1 is the Hall mobility in the grain (1), $\beta \equiv l_2/l_1$, and $\alpha \equiv \rho_1/\rho_2$.

By assuming that $\mu_1 = \mu_{\text{tot}}$, μ_m would be calculated according to Eq. (1) with appropriate values of α and β. Rice and Malloy have considered the contribution of inhomogeneity on the Hall mobility in *p*-GaN and given that the typical values of α and β are approximately 10^{-4} and 3×10^{-3}, respectively.[17] It should be noted that since impurity and defect concentrations are different in regions 1 and 2, the temperature dependence of the hole concentration and mobility in each region will necessarily follow different laws, and α will be temperature dependent. Indeed, it is very difficult to give the values of α as a function of temperature. In this case, we just give an estimated range for α of about 10^{-3}–10^{-2}, which is comparable to that of *p*-GaN. On the other hand, to estimate the value of β, the dimension of the high-resistivity region should be considered. It is well known that the grain boundaries generally contain high densities of interface states, which trap free carriers from the grains. Then the width of the depleted region at the grain boundaries must be of the order of the Debye length in grains, which, for a hole concentration of 5×10^{16} cm^{-3}, is about 15 nm. Thus l_2 must be twice the corresponding Debye length. If $l_1 \approx 300$ nm, then $\beta \approx 10^{-1}$. Thus we can obtain the curve of the measured Hall mobility for inhomogeneous films according to Eq. (1), i.e., $\mu_{m1}=0.09\mu_{\text{tot}}$ for $\alpha=10^{-2}$ and $\beta=10^{-1}$ and $\mu_{m2}=0.01\mu_{\text{tot}}$ for $\alpha=10^{-3}$ and $\beta=10^{-1}$, as shown in Fig. 1. It can be found that the experimental data favorably scatter in the area between the curves of μ_{m1} and μ_{m2}, indicating that the estimated range of α is reasonable for our *p*-type samples.

If we tentatively assume that $\alpha=3\times10^{-3}$ and $\beta=10^{-1}$, the curve of μ_m can fit the data very well, as shown in Fig. 1. Nevertheless, despite the lack of values of α as a function of temperature, we can also conclude that no matter which value it would be in the range of 10^{-3}–10^{-2} over temperatures of 85–300 K, the curve of μ_m calculated by Eq. (1) must be in the range between μ_{m1} and μ_{m2}, in agreement with the experimental data. This clearly demonstrates that besides ionized impurity and acoustic deformation potential scatterings at low temperatures and the polar optical phonon scattering at high temperatures, the effects of the inhomogeneous microstructure in *p*-type ZnO films play a more important role in determining the hole mobility. As shown by the AFM and XRD results, the *p*-type ZnO films consist of two kinds of columnar domains surrounded by grain boundaries. These boundaries generally contain fairly high densities of interface states which trap free carriers from the grains, scatter free carriers by virtue of the inherent disorder and the presence of trapped charge, and may also act as sinks for the segregation of dopant atoms.[21] Thus, the inhomogeneity of *p*-type ZnO can considerably reduce the hole mobility.

In conclusion, the temperature-dependent hole mobility in *p*-type ZnO grown on *c*-Al_2O_3 was studied both experimentally and theoretically. The experimental Hall mobility was found to be considerably lower than the calculated mobility involved in traditional scattering mechanisms. However, taking the effect of inhomogeneity on the mobility into account, the calculated mobility was in excellent agreement with the experimental data. This indicates that besides ionized impurity and acoustic deformation potential scatterings at low temperatures and the polar optical phonon scattering at high temperatures, the effects of the inhomogeneous microstructure in *p*-type ZnO films play a more important role in determining the hole mobility, including columnar grain size and grain boundaries, which were confirmed by AFM and XRD results.

This work is supported by the Key Project of the National Natural Science Foundation of China under Grant Nos. 60336020 and 50532050, the Innovation Project of Chinese Academy of Sciences, and the National Natural Science Foundation of China under Grant Nos. 60429403, 60506014, 60576040, and 10674133.

[1] D. C. Look, Mater. Sci. Eng., B **80**, 383 (2001).
[2] A. Tsukazaki, T. Onuma, M. Ohtani, T. Makino, M. Sumiya, K. Ohtani, S. F. Chichibu, S. Fuke, Y. Segawa, H. Ohno, H. Koinuma, and M. Kawasaki, Nat. Mater. **4**, 42 (2005).
[3] H. W. Liang, Y. M. Lu, D. Z. Shen, Y. C. Liu, J. F. Yan, C. X. Shan, B. H. Li, Z. Z. Zhang, J. Y. Zhang, and X. W. Fan, Phys. Status Solidi A **202**, 1060 (2005).
[4] S. J. Jiao, Z. Z. Zhang, Y. M. Lu, D. Z. Shen, B. Yao, J. Y. Zhang, B. H. Li, D. X. Zhao, and X. W. Fan, Appl. Phys. Lett. **88**, 031911 (2006).
[5] W. Liu, S. L. Gu, J. D. Ye, S. M. Zhu, S. M. Liu, X. Zhou, R. Zhang, Y. Shi, Y. D. Zheng, Y. Hang, and C. L. Zhang, Appl. Phys. Lett. **88**, 092101 (2006).
[6] W. Z. Xu, Z. Z. Ye, Y. J. Zeng, L. P. Zhu, B. H. Zhao, L. Jiang, J. G. Lu, H. P. He, and S. B. Zhang, Appl. Phys. Lett. **88**, 173506 (2006).
[7] T. Makino, A. Tsukazaki, A. Ohtomo, M. Kawasaki, and H. Koinuma, Jpn. J. Appl. Phys., Part 1 **45**, 6346 (2006).
[8] F. X. Xiu, Z. Yang, L. J. Mandalapu, D. T. Zhao, J. L. Liu, and W. P. Beyermann, Appl. Phys. Lett. **87**, 152101 (2005).
[9] D. C. Look, Semicond. Sci. Technol. **20**, S55 (2005).
[10] B. Claflin, D. C. Look, S. J. Park, and G. Cantwell, J. Cryst. Growth **287**, 16 (2006).
[11] D. A. Anderson and N. Apsley, Semicond. Sci. Technol. **1**, 187 (1986).
[12] Y. S. Jung, O. V. Kononenko, and W. K. Choi, Solid State Commun. **137**, 474 (2006).
[13] R. L. Petritz and W. W. Scanlon, Phys. Rev. **97**, 1620 (1955).
[14] A. R. Hutson, Phys. Rev. **108**, 222 (1957).
[15] J. W. Sun, Y. M. Lu, Y. C. Liu, D. Z. Shen, Z. Z. Zhang, B. H. Li, J. Y. Zhang, B. Yao, D. X. Zhao, and X. W. Fan, Solid State Commun. **140**, 345 (2006).
[16] D. C. Look, D. C. Reynolds, C. W. Litton, R. L. Jones, D. B. Eason, and G. Cantwell, Appl. Phys. Lett. **81**, 1830 (2002).
[17] A. K. Rice and K. J. Malloy, J. Appl. Phys. **89**, 2816 (2001).
[18] J. Volger, Phys. Rev. **79**, 1023 (1950).
[19] R. H. Bube, Appl. Phys. Lett. **13**, 136 (1968).
[20] J. Heleskivi and T. Salo, J. Appl. Phys. **43**, 740 (1972).
[21] J. W. Orton and M. J. Powell, Rep. Prog. Phys. **43**, 81 (1980).